PHYSICAL REVIEW B **67**, 100506(R) (2003)

Energy-dependent modulations in the local density of states of the cuprate superconductors

Degang Zhang and C. S. Ting
Texas Center for Superconductivity and Department of Physics, University of Houston, Houston, Texas 77204
(Received 15 January 2003; published 25 March 2003)

Motivated by the recent scanning tunneling microscopy (STM) experiment [J. E. Hoffman *et al.*, Science **297**, 1148 (2002)], we investigate the energy-dependent modulation of local density of states induced by a weak and extended defect in a *d*-wave superconductor. The Fourier component of the local density of states is calculated up to the first order in the defect parameters. Our numerically obtained image maps together with the energy-dependent charge modulation wave vectors at different dopings exhibit the essential features as those measured by the experiment. We also predict new modulation wave vectors in the first Brillouin zone. Hopefully, they could be verified by future STM experiments.

DOI: 10.1103/PhysRevB.67.100506 PACS number(s): 74.25.−q, 74.62.Dh, 74.72.−h

In the past year, a series of scanning tunneling spectroscopy (STM) experiments have confirmed the coexistence of charge modulation and superconductivity in $Bi_2Sr_2CaCu_2O_{8+\delta}$.[1–3] In a magnetic field, Hoffman *et al.*[1] discovered a four-cell checkerboard local density of states (LDOS) modulation localized in a small region around the vortex core. The field-induced charge modulation oriented parallel to the Cu-O bond directions is relatively strong. Subsequently, Howald *et al.*[2] also observed similar checkerboard charge modulation in absence of magnetic field for a wide range of bias voltages, but with relatively weak intensity.

Recently, Hoffman *et al.*[3] also investigated the zero-field charge modulation by employing high-resolution Fourier-transform scanning tunneling spectroscopy. They found that the period of the charge modulation depends on the energy and doping for the bias voltages below the maximum superconducting gap. With the bias voltage (doping fixed) or doping (bias voltage fixed) increasing, the LDOS modulation wave vectors oriented parallel to the $(\pm\pi,0)$ and $(0,\pm\pi)$ directions become shorter while those oriented parallel to the $(\pm\pi,\pm\pi)$ directions become longer.

A number of theoretical studies on the STM spectra have already been carried out by several authors[4–7] in attempt to explain the zero-field LDOS modulation observed by Howald *et al.*[2] There are also works[8–10] trying to understand the energy-dependent LDOS modulation observed in the zero-field STM experiment.[3] In Ref. 8, Wang and Lee proposed that the experimental observation of Hoffman *et al.*[3] is a result of the quasiparticle interference induced by an impurity with an on-site potential of moderate strength. However, these calculations[8–10] seem only able to address a limited portion of the STM experimental measurements,[3] and did not obtain the Fourier component of the LDOS along the $(\pi,0)$ and the (π,π) directions and the relations among the peaks associated with the modulation wave vectors, dopings and the bias voltages as those presented in Ref. 3.

In this work, we examine the effects of the scattering of a quasiparticle by a weak and extended defect or impurity with both hopping and pairing disorders on the Fourier transform of the LDOS. Using the first-order *T*-matrix approximation, we show that our results are consistent with all the essential features observed in the experiment of Ref. 3. In addition, we predict that modulation wave vectors existed in the first Brillouin zone, hopefully they could be verified by future STM experiments.

The Hamiltonian describing the scattering of quasiparticles from a single defect with local modifications of both hopping and pairing parameters in a *d*-wave superconductor can be written as

$$H = H_{\rm BCS} + H_{\rm imp},$$

$$H_{\rm BCS} = \sum_{\mathbf{k}\sigma} (\epsilon_{\mathbf{k}} - \mu) c^{\dagger}_{\mathbf{k}\sigma} c_{\mathbf{k}\sigma} + \sum_{\mathbf{k}} \Delta_{\mathbf{k}} (c^{\dagger}_{\mathbf{k}\uparrow} c^{\dagger}_{-\mathbf{k}\downarrow} + c_{-\mathbf{k}\downarrow} c_{\mathbf{k}\uparrow}),$$

$$H_{\rm imp} = \sum_{\langle i,j\rangle,\sigma} \delta t_{ij} c^{\dagger}_{i\sigma} c_{j\sigma} + \sum_{\langle i,j\rangle} \delta\Delta_{ij} (c^{\dagger}_{i\uparrow} c^{\dagger}_{j\downarrow} + c_{j\downarrow} c_{i\uparrow}) + (V_s + V_m) c^{\dagger}_{0\uparrow} c_{0\uparrow} + (V_s - V_m) c^{\dagger}_{0\downarrow} c_{0\downarrow}. \quad (1)$$

Here μ is the chemical potential to be determined by doping, $\epsilon_k = t_1(\cos k_x + \cos k_y)/2 + t_2 \cos k_x \cos k_y + t_3(\cos 2k_x + \cos 2k_y)/2 + t_4(\cos 2k_x \cos k_y + \cos k_x \cos 2k_y)/2 + t_5 \cos 2k_x \cos 2k_y$, where $t_{1-5} = -0.5951, 0.1636, -0.0519, -0.1117, 0.0510$ eV. The band parameters are taken from those of Norman *et al.*[11] for $Bi_2Sr_2CaCu_2O_{8+\delta}$, and the lattice constant a is set as $a=1$. The order parameter away from the impurity is given by $\Delta_{\mathbf{k}} = \Delta_0(\cos k_x - \cos k_y)/2$.

Without loss of generality, at the impurity or defect site, we assume an on-site potential consisting of a nonmagnetic part V_s and a magnetic part V_m. The defect also induces a weak local modification in the hopping, δt, to the nearest-neighor sites, and a suppression of the superconductivity order parameter on the four bonds connected to the impurity site, $\delta\Delta_1$, and on the other 12 bonds conncted to the nearest-neighbor sites, $\delta\Delta_2$.

The Hamiltonian (1) has in fact been successfully applied by Tang and Flatte[12] to explain the resonant STM spectra for Ni impurities in $Bi_2Sr_2CaCu_2O_{8+\delta}$. In the present situation, no resonances in LDOS have been observed in the recent STM experiments.[2,3] So it is reasonable to assume that the on-site potentials (V_s and V_m) and the modifications in hopping and pairing parameters (δt, $\delta\Delta_1$, and $\delta\Delta_2$) are all weak and have approximately the same order of magnitude. 'In order to compare with the measurements in the STM

experiment,[3] we investigate three different hole doping cases: underdoping (10%) with $\Delta_0 = 50$ meV, optimal doping (15%) with $\Delta_0 = 44$ meV, and overdoping (17%) with $\Delta_0 = 37$ meV. Here we shall not discuss the issue as to why the underdoped case has a higher Δ_0 value, and simply accept it as an experimental fact.[3]

Our method to solve the Hamiltonian (1) and to obtain the LDOS is the standard Bogoliubov transformation plus Green's-function technique. When $\delta t, \delta\Delta_1, \delta\Delta_2, V_s$, and V_m are all small, keeping the leading term in the T-matrix approach should be a good approximation. The Fourier component of the LDOS obtained in such an approximation can be shown to have the following form:

$$\rho_{\mathbf{q}}(\omega) = -\frac{2}{\pi N^2}\sum_{\mathbf{k}}\sum_{\nu,\nu'=0,1}\{[2\,\delta t A(\mathbf{k},\mathbf{q}) + V_s]\alpha_{\nu\nu'}(\mathbf{k},\mathbf{q}) + 2[\,\delta\Delta_1 B(\mathbf{k},\mathbf{q}) + \delta\Delta_2 C(\mathbf{k},\mathbf{q})]\beta_{\nu\nu'}(\mathbf{k},\mathbf{q})\} \times \mathrm{Im}[G^0_{\mathbf{k}\nu}(i\omega_n)G^0_{\mathbf{k}+\mathbf{q}\nu'}(i\omega_n)]|_{i\omega_n\to\omega+i0^+}, \quad (2)$$

where N is the number of sites in the lattice, $A(\mathbf{k},\mathbf{q}) = \cos k_x + \cos k_y + \cos(k_x+q_x) + \cos(k_y+q_y)$, $B(\mathbf{k},\mathbf{q}) = \cos k_x - \cos k_y + \cos(k_x+q_x) - \cos(k_y+q_y)$, $C(\mathbf{k},\mathbf{q}) = \cos(k_x + 2q_x) - \cos(k_y+q_x+q_y) - \cos(k_y-q_x+q_y) + \cos(k_x+q_x+q_y) + \cos(k_x+q_x-q_y) - \cos(k_y+2q_y) + \cos(k_x-q_x) + \cos(k_x-q_y) - \cos(k_y-q_x) - \cos(k_y-q_y) + \cos(k_x+q_y) - \cos(k_y+q_x)$, $\alpha_{\nu\nu'}(\mathbf{k},\mathbf{q}) = \xi^2_{\mathbf{k}\nu}\xi^2_{\mathbf{k}+\mathbf{q}\nu'} - (-1)^{\nu+\nu'}\xi_{\mathbf{k}\nu}\xi_{\mathbf{k}\nu+1}\xi_{\mathbf{k}+\mathbf{q}\nu'}\xi_{\mathbf{k}+\mathbf{q}\nu'+1}$, $\beta_{\nu\nu'}(\mathbf{k},\mathbf{q}) = (-1)^{\nu}\xi_{\mathbf{k}\nu}\xi_{\mathbf{k}\nu+1}\xi^2_{\mathbf{k}+\mathbf{q}\nu'} + (-1)^{\nu'}\xi^2_{\mathbf{k}\nu}\xi_{\mathbf{k}+\mathbf{q}\nu'} \times \xi_{\mathbf{k}+\mathbf{q}\nu'+1}$, $G^0_{\mathbf{k}\nu}(i\omega_n) = 1/[i\omega_n - (-1)^{\nu}E_{\mathbf{k}}]$ is the bare Green's function, $E_{\mathbf{k}} = \sqrt{(\epsilon_{\mathbf{k}}-\mu)^2+\Delta^2_{\mathbf{k}}}$, $\xi^2_{\mathbf{k}\nu} = [1 + (-1)^{\nu}(\epsilon_{\mathbf{k}}-\mu)/E_{\mathbf{k}}]/2$, and $\xi_{\mathbf{k}0}\xi_{\mathbf{k}1} = \Delta_{\mathbf{k}}/(2E_{\mathbf{k}})$.

It is noted that V_m is absent from Eq. (2) because there is no first-order contribution from the magnetic potential. In the present study, we base our numerical calculation on a finite lattice of 800×800 lattice sites with the defect at the center. For simplicity, we choose $2\,\delta t = V_s = -2\,\delta\Delta_1 = -4\,\delta\Delta_2$, and assume that all these parameters are small such that the first-order T-matrix approximation is valid. The advantage of this first-order approximation is that the states of quasiparticle before and after scattering from the defect are clearly distinguishable. In our calculation, we also introduce a finite lifetime broadening $\gamma = 2$ meV to the quasiparticle Green's function to smooth our data points by replacing $\omega + i0^+$ with $\omega + i\gamma$ in Eq. (2).

It is well known that the quasiparticles in a d-wave superconductor are Bloch wave states. In the presence of electron-impurity interactions, elastic scattering mixes those eigenstates of the quasiparticle with the same energy but different momentum. For example, if a quasiparticle with energy $E_{\mathbf{k}}$ is excited at the point O in Fig. 1(a), after being scattered by the defect, the quasiparticle energy becomes $E_{\mathbf{k}+\mathbf{q}}$ ($\equiv E_{\mathbf{k}}$). There are six nonequivalent $\mathbf{q}$ vectors as shown in Fig. 1(a). The variation in the magnitudes of these $\mathbf{q}$ vectors with ω would lead to energy-dependent LDOS modulations.

According to Eq. (2), we plot the image map of the Fourier component of LDOS in Fig. 1(b) for the optimally doped case at fixed $\omega = -16$ meV in the first Brillouin zone. In Fig. 1(b) we are able to clearly identify four of the six $\mathbf{q}$ vectors as shown in Fig. 1(a) from the positions of the peaks (or local maxima). The four peaks with relatively weak intensity along $(\pm\pi,0)$, $(0,\pm\pi)$ directions and the four peaks with relatively strong intensity along $(\pm\pi,\pm\pi)$ directions as shown in Fig. 1(b), are respectively, related to $\mathbf{q}_A$ and $\mathbf{q}_B$ in Fig. 1(a), and both of them have been observed in Ref. 3. In addition, we predict that there are another eight weak peaks corresponding to $\mathbf{q}_C$. At the four corners of the first Brillouin zone, there are four extended weak peak arcs generated from the quasiparticle interference between the banana-shaped equal-energy contours of the diagonal Fermi surfaces connected by $\mathbf{q}_D$. Since the peaks at $\mathbf{q}_B$ have the highest intensity, we expect that the real space LDOS image at $\omega = -16$ meV should have a checkerboard pattern oriented along 45° to the Cu-O bonds with a period close to $5a$.

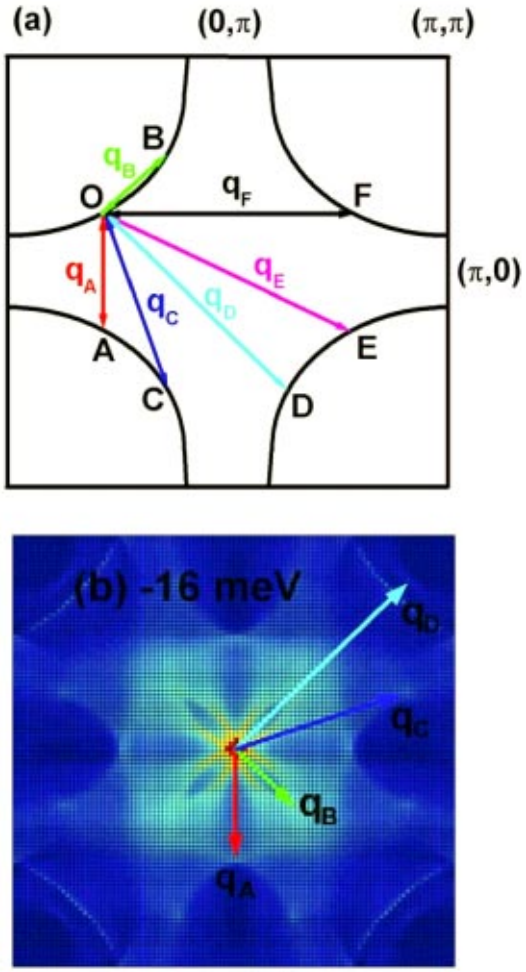

FIG. 1. (a) Schematic Fermi surface of high-T_C cuprate superconductor. The modulation wave vectors connecting different points of the Fermi surface with the same energy gap are shown. (b) The Fourier component of LDOS $\rho_{\mathbf{q}}(\omega)$ for the optimally doped case at $\omega = -16$ meV in the first Brillouin zone (i.e., $-\pi < q_x, q_y \leq \pi$).

In Figs. 2(a)–2(c), the $\mathbf{q}$-space LDOS maps for the optimally doped case are also presented at $\omega = 0, -12, -20$ meV in the first Brillouin zone. We noticed that the detailed image of the map depends on the magnitude of ω,

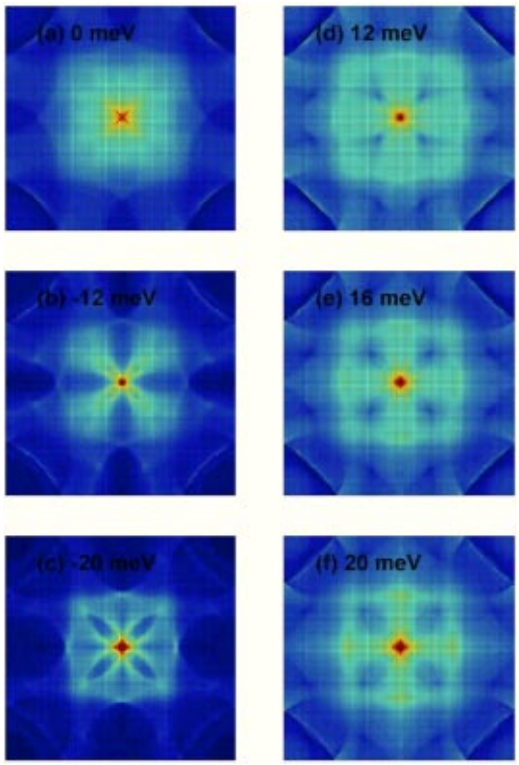

FIG. 2. The Fourier component of LDOS $\rho_{\mathbf{q}}(\omega)$ for the optimally doped case at different energy shown in each panel in the first Brillouin zone.

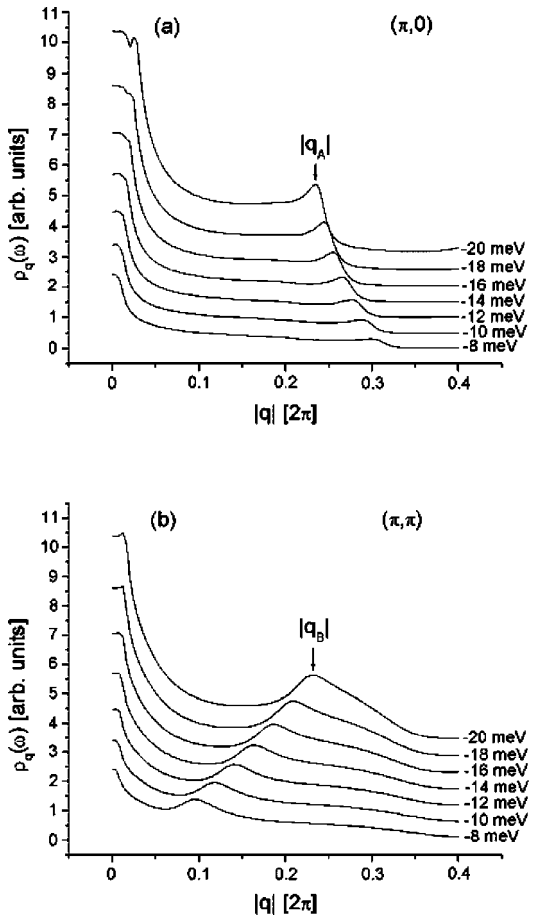

FIG. 3. $\rho_{\mathbf{q}}(\omega)$ versus $|\mathbf{q}|$ for the optimally doped case along (a) the $(\pi,0)$ direction and (b) the (π,π) direction are shown for seven quasiparticle energies. The data are shifted vertically relative to each other by 0.5 unit for clarity.

when it increases, $|\mathbf{q}_A|$ becomes shorter while $|\mathbf{q}_B|$, $|\mathbf{q}_C|$, and $|\mathbf{q}_D|$ become longer. In Fig. 2(c) with $\omega=-20$ meV, the intensity of the peaks at $\mathbf{q}_A$ is catching up with that at $\mathbf{q}_B$ as compared with the case of $\omega=-16$ meV. And it is expected to become dominant at a larger $|\omega|$, there, the real space LDOS image would have a checkerboard pattern oriented along the Cu-O bonds with a period close to $4a$. This is consistent with the experiment in Ref. 3.

It needs to be mentioned that the peaks corresponding to the remaining two modulation wave vectors $\mathbf{q}_E$ and $\mathbf{q}_F$ [see Fig. 1(a)] are clearly missing in these maps [see Fig. 1(b), and Figs. 2(a)–2(c)]. At $\omega=0$ meV, $\mathbf{q}_D$ and $\mathbf{q}_E$ are equivalent and a small arc peak is created at them, but the resolution of the map is not clear enough to show the existence of $\mathbf{q}_F$ (i.e., $\mathbf{q}_A$ and $\mathbf{q}_C$). For $\omega=-12,-16,-20$ meV, both of these wave vectors do not appear in the first Brillouin zone, but they may yield local peaks in the second Brillouin zone. So far the experiments have not yet been performed in this region, their effects will not be considered in the present study. But we do expect that the peaks associated with these wave vectors would show up when the boundary of our calculation is expanded beyond that of the first Brillouin zone. Although our image map at $\omega=-12$ meV is similar to the corresponding one in Ref. 8, there still exist some fundamental differences between these two results. For example, the bright spots at points $(\pm\pi,\pm\pi)$ that appeared in the image maps of Ref. 8 close to $\omega=-20$ meV did not show up in our maps. These bright spots are probably due to the impurity resonant states, which were not observed by the STM experiments. Moreover, in Ref. 8, only the effect due to $\mathbf{q}_A$ and $\mathbf{q}_B$ was addressed.

At $\omega=12,16,20$ meV, the maps of the Fourier component of LDOS for the optimally doped case are shown in Figs. 2(d)–2(f). The modulation wave vectors are identical to those for the negative ω. But the Fourier component of LDOS at $\mathbf{q}_B$, $\mathbf{q}_C$, and $\mathbf{q}_D$ shows a local minimum intensity. This is primarily due to the destructive interference between the opposite phases carried by the quasiparticles before and after scattering. This destructive interference has also been observed at $\omega=16,22$ meV in the STM experiment of Ref. 3 [see Figs. 2(c) and 2(d) there]. Obviously, the wave vectors at extreme (maximum or minimum) values of $\rho_{\mathbf{q}}(\omega)$ for the positive ω coincide with those in Fig. 1(b), Figs. 2(b) and 2(c). In addition, we also found that in the higher-energy region close to the maximum of the superconductivity gap, our image maps become blurred. The reason is not clear to us, but it might be due to many competing modulation wave vectors gaining strengths on the same banana-shaped equal-energy contour of the Fermi surface.

In order to compare with the experimental curves in Ref. 3, Fig. 3 shows the Fourier component of LDOS, respectively, along $(\pi,0)$ [Fig. 3(a)] and (π,π) [Fig. 3(b)] direc-

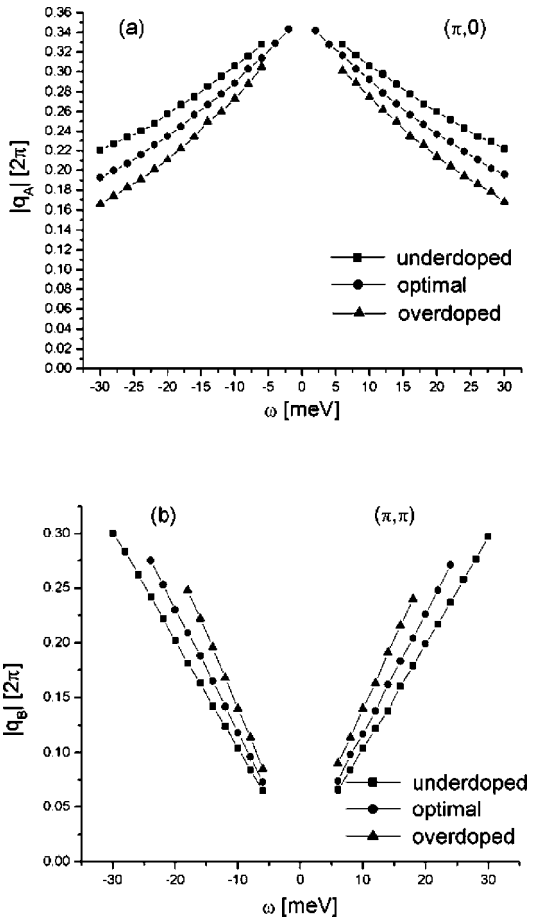

FIG. 4. The modulation wave vectors versus energy along (a) the $(\pi,0)$ direction and (b) the (π,π) direction are plotted for underdoped, optimally and overdoped cases.

tions as a function of $|\mathbf{q}|$ up to $|\mathbf{q}|=0.4$ (in unit of 2π) for the optimally doped sample. Along $(\pi,0)$ direction, the peak of $\rho_{\mathbf{q}}(\omega)$ associated with $\mathbf{q}_A$ moves slowly towards the origin when energy increases. In contrast, along (π,π) direction, the peak of $\rho_{\mathbf{q}}(\omega)$ associated with $\mathbf{q}_B$ moves rapidly away from the origin. This energy-dependent position of the peaks at $\mathbf{q}_A$ or $\mathbf{q}_B$ is responsible for the checkerboard pattern with an energy-dependent period as observed in Ref. 3. In the presence of other competing modulation wave vectors at higher energy, the LDOS image pattern could be dramatically modified.

We also study the effects of doping on $\rho_{\mathbf{q}}(\omega)$. Figure 4 shows the peak positions at $|\mathbf{q}_A|$ along $(\pi,0)$ direction [Fig. 4(a)] and at $|\mathbf{q}_B|$ along (π,π) direction [Fig. 4(b)] as a function of ω at three different dopings. As energy is fixed, $|\mathbf{q}_A|$ becomes smaller while $|\mathbf{q}_B|$ becomes larger as the doping is increased. It is apparent that the results in Figs. 3 and 4 are in qualitative agreement with those experimental curves in Ref. 3.

In summary, we have studied the energy-dependent LDOS modulations in *d*-wave superconductors with the presence of an extended defect using the Bogoliubov transformation plus the Green's-function approach. The changes in pairing order parameter and hopping terms due to such an extended defect generate some **k**- and **q**-dependent terms as shown in Eq. (2), which seem to be essential for obtaining the curves in Figs. 3 and 4. In addition, we also discover new modulation wave vectors $\mathbf{q}_C$ and $\mathbf{q}_D$ in the first Brillouin zone. Hopefully, they could be observed in future experiments. Since the effects of the modulation wave vectors in the second Brillouin zone have not been carefully examined, we are not able to obtain the complete LDOS images in real space by the Fourier transform. This is an important problem and should constitute a subject for future investigation.[13] We note that for the system with many random impurities, the modulation wave vectors are the same with those in a single-impurity case. This means that the peak positions of the Fourier component of the LDOS remain unchanged. We also note that using the triangular relation $\mathbf{q}_A+\mathbf{q}_B=\mathbf{q}_C$, the Fermi surface and the energy gap could be mapped out.

Our predicted new modulation wave vectors were recently observed by McElroy *et al.*[14] in their STM experiment.

We wish to thank Professor J. C. Davis for sending us Ref. 3 before its publication, and H. Y. Chen, M. Shaw, Y. Chen, and Professor S. H. Pan for useful discussions. This work has been supported by the Texas Center for Superconductivity at the University of Houston and by the Robert A. Welch Foundation.

[1] J.E. Hoffman, E.W. Hudson, K.M. Lang, V. Madhavan, H. Eisaki, S. Uchida, and J.C. Davis, Science **295**, 466 (2002).
[2] C. Howald, H. Eisaki, N. Kaneko, and A. Kapitulnik, cond-mat/0201546 (unpublished).
[3] J.E. Hoffman, K. McElroy, D.-H. Lee, K.M. Lang, H. Eisaki, S. Uchida, and J.C. Davis, Science **297**, 1148 (2002).
[4] Y. Chen, H.Y. Chen, and C.S. Ting, Phys. Rev. B **66**, 104501 (2002).
[5] D. Podolsky, E. Demler, K. Damle, and B.I. Halperin, cond-mat/0204011, Phys. Rev. B (to be published 1 March 2003).
[6] M. Vojta, Phys. Rev. B **66**, 104505 (2002).
[7] Degang Zhang, Phys. Rev. B **66**, 214515 (2002).
[8] Qiang-Hua Wang and Dung-Hai Lee, Phys. Rev. B **67**, 020511 (2003).
[9] J.H. Han, cond-mat/0206284, Phys. Rev. B (to be published 1 March 2003).
[10] A. Polkovnikov, M. Vojta, and S. Sachdev, Phys. Rev. B **65**, 220509 (2002).
[11] M.R. Norman, M. Randeria, H. Ding, and J.C. Campuzano, Phys. Rev. B **52**, 615 (1994).
[12] Jian-Ming Tang and M.E. Flatte, Phys. Rev. B **66**, 060504 (2002).
[13] Degang Zhang and C. S. Ting (unpublished).
[14] K. McElroy *et al.* (unpublished).